MOLECULAR AND CELLULAR BIOLOGY, May 2006, p. 3455–3467 Vol. 26, No. 9
0270-7306/06/$08.00+0 doi:10.1128/MCB.26.9.3455–3467.2006

FATP1 Is an Insulin-Sensitive Fatty Acid Transporter Involved in Diet-Induced Obesity

Qiwei Wu,[1] Angelica M. Ortegon,[2] Bernice Tsang,[2] Holger Doege,[1] Kenneth R. Feingold,[3] and Andreas Stahl[1,2]*

Palo Alto Medical Foundation Research Institute, 795 El Camino Real, Palo Alto, California 94301[2]; Division of GI/Hepatology, Stanford University School of Medicine, Stanford, California 94305[1]; and Department of Veterans Affairs, 4150 Clement St., San Francisco, California 94121[3]

Received 24 October 2005/Returned for modification 22 November 2005/Accepted 9 February 2006

Fatty acid transport protein 1 (FATP1), a member of the FATP/Slc27 protein family, enhances the cellular uptake of long-chain fatty acids (LCFAs) and is expressed in several insulin-sensitive tissues. In adipocytes and skeletal muscle, FATP1 translocates from an intracellular compartment to the plasma membrane in response to insulin. Here we show that insulin-stimulated fatty acid uptake is completely abolished in FATP1-null adipocytes and greatly reduced in skeletal muscle of FATP1-knockout animals while basal LCFA uptake by both tissues was unaffected. Moreover, loss of FATP1 function altered regulation of postprandial serum LCFA, causing a redistribution of lipids from adipocyte tissue and muscle to the liver, and led to a complete protection from diet-induced obesity and insulin desensitization. This is the first in vivo evidence that insulin can regulate the uptake of LCFA by tissues via FATP1 activation and that FATPs determine the tissue distribution of dietary lipids. The strong protection against diet-induced obesity and insulin desensitization observed in FATP1-null animals suggests FATP1 as a novel antidiabetic target.

The metabolic syndrome (syndrome X), characterized by obesity, hyperglycemia, hyperinsulinemia, hypertension, and dyslipidemia, is a major cause of death worldwide, and insulin resistance is a hallmark of these disorders (40). The mechanism by which insulin resistance occurs is unknown but is likely to be related to alterations in lipid and fatty acid metabolism (6). Chronic elevation of plasma free fatty acid levels is commonly associated with impaired insulin-mediated glucose uptake (46), obesity, and type 2 diabetes (36). While long-chain fatty acids (LCFAs) can signal through G-protein-coupled receptors on the plasma membrane of certain cell types (47), they typically must first cross the plasma membrane and enter the cell to elicit their effects. If, and how, insulin can acutely regulate this process in adipose, muscle, and cardiac tissues is poorly understood.

Uptake of unesterified LCFAs into mammalian cells occurs through both a passive flip-flop and a saturable, protein-mediated mechanism. At physiological serum-to-albumin ratios, the concentration of unbound fatty acids is low (7.5 nM) (37), and over 90% of the LCFA uptake into tissues, such as adipocytes, occurs via the saturable pathway (52). Besides adipose tissue, other organs such as the intestine (19, 51), liver (49), and heart (42, 50) express a saturable and specific LCFA transport system (3). Several membrane proteins that increase the uptake of LCFAs when overexpressed in cultured mammalian cells have been identified. The most prominent and best characterized of these are FAT/CD36 (10), long-chain fatty acyl coenzyme A (acyl-CoA) synthetases (9, 39), and fatty acid transport proteins (FATPs; solute carrier family 27). Six FATP genes are found in human and mouse genomes (FATP1 through -6, Slc271 to -6) (43). FATP1 was the first family member identified (39) and is thus far the best studied. Human and murine FATP1 is a 71-kDa transmembrane protein and is the major FATP in adipose tissue (39). It is also found in skeletal muscle and to a lesser extent in heart tissue (5, 24, 39). FATP1 displays acyl-CoA activity (12), but it remains unclear if this enzymatic activity is required to drive fatty acid uptake (58).

Insulin's actions on glucose uptake have been the subject of intense research over several decades that has demonstrated that it predominantly decreases glucose concentrations by a dual mechanism, i.e., suppressing hepatic glucose release and increasing glucose uptake through the translocation of the insulin-sensitive glucose transporter GLUT4 (53). While insulin also suppresses the release of fatty acids into the circulation by inhibiting hormone-sensitive lipase in adipocytes, little is known about whether it also increases protein-mediated uptake. We have previously shown that, in adipocytes, insulin induces translocation of FATP1 from an intracellular perinuclear compartment, where it colocalizes with the insulin-sensitive glucose transporter GLUT4 to the plasma membrane (44). In contrast, neither the highly related FATP4 (61% sequence identity) nor CD36 showed a similar dynamic localization in the same cells (44). Insulin-induced FATP1 translocation coincides with increased LCFA uptake in fat (44), suggesting that hormonal regulation of FATP1 activity may play an important role in energy homeostasis. However, insulin affects fatty acid metabolism on several levels, including lipolysis and β-oxidation, and it remained unclear how much of the insulin-induced increase in LCFA uptake is due to enhanced transport versus changes in subsequent intracellular events. To address these questions, we have generated FATP1-null mice (28). Initial characterization of these mice focused primarily on alterations in insulin sen-

* Corresponding author. Mailing address: Palo Alto Medical Foundation Research Institute, Ames Building, 795 El Camino Real, Palo Alto, CA 94301. Phone: (650) 614-3293. Fax: (650) 329-9114. E-mail: astahl@stanford.edu.

sitivity in skeletal muscle using hyperinsulinemic-euglycemic clamp studies following lipid injections or short-term high-fat challenges (28). Importantly, these studies showed that loss of FATP1 led to reduced skeletal muscle lipid accumulation and improved insulin sensitivity after lipid challenges, highlighting the importance of excessive intramuscular triglyceride (TG) in the etiology of type 2 diabetes (28). However, the contribution of FATP1 to basal and insulin-stimulated LCFA uptake as well as its role in the development of chronic high-fat-induced obesity/insulin resistance remained unresolved. Here we used FATP1-knockout (KO) mice to study insulin-mediated LCFA uptake and to demonstrate that the dynamic regulation of fatty acid uptake by peripheral tissues depends on an insulin-sensitive FATP1 compartment. Loss of this mechanism results in a redistribution of postprandial lipids from adipocytes and muscle to the liver, resulting in protection from chronic high-fat diet-induced insulin desensitization.

MATERIALS AND METHODS

Antibodies and reagents. BODIPY (4,4-difluoro-3a,4a-diaza-s-indacene) fatty acid (C_1-BODIPY-C_{12}) was obtained from Molecular Probes, and [^{14}C]oleic acid and 2-deoxy-D-[1-^{3}H]glucose (2-DG) were purchased from American Radiolabeled Chemicals. NSC119889 and NSC154020 were from Calbiochem (San Diego, CA). Wortmannin, U0126, PP2, and Go 6850 were from Tocris Bioscience (Ellisville, MO). Polyclonal antisera against the C termini of FATP1 to -6 were raised as described previously (44), mouse monoclonal anti-Glut4 and anti-caveolin 3 were purchased from BD Pharmingen, and the mouse monoclonal anti-CD36/FAT antibody was a gracious gift from Maria Febbraio.

Skeletal muscle fractionation. One gram of insulin-treated and untreated flash-frozen soleus tissue was thawed in 30 ml of ice-cold sucrose buffer (250 mM sucrose, 20 mM HEPES-Tris, 1 mM EDTA, 100 μM phenylmethylsulfonyl fluoride, pH 7.4), minced with scissors, and homogenized with a Polytron device (setting 3; 30 s). This homogenate was filtered through two layers of cheesecloth to remove residual connective tissue and centrifuged (3,000 × *g* for 10 min at 4°C). The pellet was saved for preparation of the plasma membrane-enriched fraction. The resulting pellet was washed twice, resuspended in 10 mM Tris-HCl (ratio of 30 ml to 1 g [wt/vol] of the original skeletal muscle), and homogenized using a Teflon pestle. The suspension was transferred to a glass beaker, a 9- by 25-mm-diameter Teflon-coated magnet was added to the beaker, and the beaker was covered with Parafilm and stored at 4°C for 16 h. Thereafter, 50 mM lithium bromide (LiBr; 200 μl/10 ml of the suspension) was added to the beaker and magnetically stirred (setting 3; 2.5 h) to extract all contractile elements. The LiBr-treated suspension was transferred to a centrifuge tube, diluted in 20 ml of 10 mM Tris-HCl, and centrifuged (10,000 × *g* for 10 min at 4°C). The pellet was resuspended in 10 ml of the 10 mM Tris-HCl and centrifuged (6,000 × *g* for 10 min at 4°C). The pellet obtained was resuspended in 25% potassium bromide (KBr; 15 ml per 1 g [wt/vol] of muscle), followed by centrifugation (10,000 × *g* for 30 min at 4°C). The KBr-treated pellet was washed once with 250 mM sucrose buffer and was recentrifuged (17,000 × *g* for 20 min at 4°C) to obtain the final plasma membrane-enriched pellet. This pellet was resuspended in 500 μl of sucrose buffer and fractionated by a continuous Percoll gradient procedure (7). In the resulting Percoll-free fractionated samples, the protein content was determined by the bicinchoninic acid method, and 10 μg of each fraction was subjected to sodium dodecyl sulfate-polyacrylamide gel electrophoresis and identified by Western blotting. Western blot signals were quantified by densitometry.

Subcellular localization of FATP1 in skeletal muscle. Soleus muscle from overnight fasted mice was dissected 30 min after intraperitoneal injection of saline or 0.75 U insulin per kg of body weight. Muscle strips were fixed in 2% paraformaldehyde, thick sectioned (15 μm to 40 μm), and stained with antibodies as previously described for FATP4 (45). Sections were examined with a Zeiss LSM10 confocal microscope. Three-dimensional reconstructions of confocal image stacks were performed using Volocity (Improvision, England).

Cell culture and [^{14}C]oleate uptake assay. 3T3-L1 fibroblasts (ATCC) were grown in Dulbecco modified Eagle medium (DMEM) containing 10% fetal bovine serum (FBS) and 1% penicillin-streptomycin (DMEM-FBS). Differentiated cells were prepared as described previously. In short, 3T3-L1 fibroblasts were grown 2 days after confluence in DMEM-FBS and then for 2 days in DMEM-FBS supplemented with 0.83 μM insulin, 0.25 μM dexamethasone, and 0.25 mM isobutylmethylxanthine. The medium was then changed to DMEM-FBS supplemented with 0.83 μM insulin for 2 days only, and then cells were maintained in DMEM-FBS alone for a further 3 to 5 days. Differentiated cells (at least 90% of cells showed lipid droplets) were used on day 8 after initiation of differentiation.

3T3-L1 adipocytes were detached with trypsin-EDTA and seeded onto a 24-well plate at ~10,000 cells/well in 500 μl of DMEM-FBS the day before assay. After 4 h of preincubation with deprivation of serum, cells were treated with inhibitors (2× 50% inhibitory concentration [IC_{50}]) and insulin (100 nM) (30 min each at 37°C). Then each well was replaced with 200 μl fatty acid uptake solution (50 μM [^{14}C]oleate in Hanks' balanced salt solution [HBS] with 0.1% fatty-acid-free bovine serum albumin [BSA]) for 5 min followed by washing with cold HBS. The cells were lysed in 250 μl radioimmunoprecipitation assay buffer and 75 μl supernatant of lysate used for scintillation count, and counts per minute were normalized by protein concentration of each lysate.

Preparation of primary cells. Primary adipocytes were prepared from epididymal fat pads as previously described (44), and hepatocytes were isolated by a dual perfusion method (48). Mouse ventricular cardiomyocytes were prepared essentially as described previously (8). Mice were subjected to overnight fasting so as to lower systemic insulin levels. The isolated cells were allowed to recover for ~2 h at room temperature in Krebs-Henseleit bicarbonate medium supplemented with 1.0 mmol/liter $CaCl_2$ and 2% (wt/vol) BSA and equilibrated with 95% O_2 and 5% CO_2 at 37°C. Only when >80% of the cells had a rod-shaped appearance and excluded trypan blue were they used for subsequent fatty acid uptake studies.

Fluorescent fatty acid and [^{14}C]oleic acid uptake assay. Fluorescence-activated cell sorter-based short-term (1-min) fatty acid uptake assays with primary adipocytes, hepatocytes, and cardiomyocytes were performed as previously described (23, 38, 41). Long-chain fatty acid uptake assays with soleus muscle were performed by incubating muscle strips in RPMI with 50 nM insulin for 30 min or without. Each muscle strip was then dipped into HBS containing 0.2% fatty-acid-free BSA, 50 μM [^{14}C]oleic acid (BSA, 55 mCi/mmol) for 1 min. After a thorough washing with ice-cold 0.2% BSA solution, muscle strips were homogenized and radioactivity in supernatants was determined by β-scintillation counting and normalized to protein amount.

Deoxyglucose uptake. A 2-DG uptake assay with soleus muscle was done simultaneously with fatty acid uptake by adding 2-deoxy-D-[1-^{3}H]glucose to a final concentration of 0.1 mmol/liter to the uptake mixture.

Diet studies. FATP1-null mice were generated as previously described (28). For diet studies, 8-week-old male mice housed separately were fed ad libitum a high-fat diet containing 60% fat (D12492; Research Diets, NJ) or a low-fat diet (D12450) containing 10% fat. Weight was measured weekly, and food intake was measured twice a week. Glucose concentrations were monitored with a glucometer (Bayer, NY) using whole blood collected from transversely sectioned tails. Standard glucose tolerance tests (1) were performed in which mice fasted for 10 h before receiving an intraperitoneal injection of 2 mg of glucose per kg of body weight in unanesthetized mice following a 12-hour fast. Circulating glucose levels were then measured at indicated time points. Insulin tolerance tests were performed similarly by injecting 0.75 U insulin per kg body weight.

Lipid gavage. Mice were given an intragastric 200-μl olive oil bolus containing 2 μCi [^{14}C]oleic acid. Before (t = 0) and at 30, 60, 120, and 240 min after administration, blood samples (75 μl) were taken by orbital eye bleeding and tissues were harvested after the last time point. ^{14}C content was measured by scintillation counting and normalized to mg protein content for tissues or μl volume for serum.

Serum analysis. Serum free fatty acids and triglyceride concentrations were measured with colorimetric assays (Wako Chemicals, VA). Levels of plasma glucose were determined enzymatically using a commercially available kit (Thermo Electron, Australia). Plasma insulin levels were determined by enzyme-linked immunoassay using a mouse insulin kit (Alpco Diagnostics, NH). Fasting plasma leptin, adiponectin, and resistin levels were measured by enzyme-linked immunosorbent assay (Linco Research, MO).

Lipoprotein separation by FPLC. One hundred fifty microliters serum from each animal in the feeding study (five male animals per group) was pooled according to diet and genotype and centrifuged twice at full speed. Total cholesterol was determined as for serum samples. Two hundred microliters of each serum pool was then applied to a fast protein liquid chromatograph (FPLC) (Pharmacia, Sweden), separated on a Superose 6 column (HR 16), and eluted with (wt/vol) 0.9% NaCl, 0.01% Tris, 0.01% EDTA, 0.02% sodium azide, pH 7.6. Up to 40 2-ml fractions were collected for each sample and assayed for protein (A_{280}) and cholesterol. Cholesterol concentrations were plotted versus fraction number. Peaks were automatically identified, integrated, and expressed as per-

TABLE 1. Nucleotide sequences of primers and probes used in this study

Gene	Forward	Probe	Reverse
PPAR-α	CGATGCTGTCCTCCTTGATGA	AAAGACGGGATGCTGATCGCGTACG	CTCGCGTGTGATAAAGCCATT
SREBP-1	CCAGAGGGTGAGCCTGACAA	AATCAGGACCATGCCGACCTCTAGTGG	AGCCTCTGCAATTTCCAGATCT
PGC-1	CATTTGATGCACTGACAGATGGA	CCGTGACCACTGACAACGAGGCC	GTCAGGCATGGAGGAAGGAC
FABP1 (liver)	CCAGGAGAACTTTGAGGCCATTC	TGAAGGCAATAGGTCTGCCCGAGGA	TGTCCTTCCCTTTCTGGATGA
CPT1	TGCAAAGATCAATCAATCGGACCC	ACACCACTGGCCGCATGTCAAGC	ACGCCACTCACGATGTTCTTC
UCP2	GTTGCCCGTAATGCCATTG	CAACTGTGCTGAGCTGGTGACCTATGACC	TTGGCTTTCAGGAGAGTATCTTTGAT
FATP5	TGGGCAGAAGCTATACCAGCAT	CCGCTCCTGGCTCCCTGCCTA	GCCGTGACTTTACCAGCTTGT
FATP2	CGGCCCAGGATGTCATCTAT	CGCTCATGATCGGCCTTCACGG	AAAGCTAAAGTAGCCCCAACCA
FAT/CD36	TTCACGGGCGTCCAGAA	TTCAGCAGGATCCATCTGGTGGACAA	GATCTTGCTGAGTCCGTTCCA

TABLE 2. FATP expression and insulin-stimulated LCFA uptake by tissues and cell lines[a]

FATP	Expression level[b] in tissue (insulin-induced LCFA uptake [% unstimulated]):				
	White adipose tissue (225)	Soleus muscle (190)	Cardiomyocytes (170)	Hepatocytes (100)	Enterocytes (90)
FATP1	+++	+++	+	−	−
FATP2	−	−	−	+++	−
FATP3	+	+	+	++	−
FATP4	++	++	++	+	+++
FATP5	−	−	−	+++	−
FATP6	−	−	+++	−	−

[a] FATP expression by tissues was determined by direct comparison using antibodies specific for FATP1 to -6. Fatty acid uptake after 30 min of incubation with or without 50 nM insulin was determined by either fluorescent fatty acid or [^{14}C]oleic acid uptake assays. Since different antisera were used, absolute expression can be compared only among tissues for each FATP.

[b] −, no expression; + to +++, lowest to highest expression levels, respectively.

centage of total signal. Absolute cholesterol amounts for very low density lipoprotein (VLDL), low-density lipoprotein (LDL), and high-density lipoprotein were calculated by multiplying the total plasma cholesterol value by the volume percentage of these specific fractions.

Tissue triglyceride analysis. Liver and skeletal muscle samples were powdered in liquid nitrogen, and total lipids were extracted by the Folch method (16). Total triglycerides were assayed using a colorimetric kit (Thermo Electron, Australia).

Fatty acid oxidation in liver slices. Liver slices (0.5 mm thick) were prepared using a McIlwain tissue slicer and placed in 25-ml Erlenmeyer center-well flasks with 2 ml Krebs-Ringer phosphate buffer. [^{14}C]oleic acid bound to fatty-acid-free BSA in Krebs-Ringer phosphate buffer was added to a final concentration of 0.5 mM and 0.15 mM, respectively, and equilibrated for 30 s with a humidified 95%/5% O_2/CO_2 gas mix. Flasks were then capped with a rubber stopper containing a centered well enclosing a loosely folded filter paper moistened with 0.2 ml of 1 N NaOH solution. After incubation for 4 h at 37°C, the reaction was stopped by injecting 0.2 ml of H_2SO_4 (1 M), and the radioactivity trapped in the filter paper was determined by scintillation counting.

Real-time PCR. Primers and a TaqMan 6-carboxyfluorescein probe for selected genes were designed using Primer Express software (Applied Biosystems, CA). Pooled total liver RNA samples of the FATP1$^{-/-}$ and littermate wild-type mice, either on a regular diet or on a high-fat diet, were prepared using an RNeasy Mini Kit (QIAGEN, CA). One microgram of total RNA was reverse transcribed in a total volume of 20 μl using the GeneAmp RNA PCR kit (Applied Biosystems) following the manufacturer's instructions. Quantitative real-time reverse transcription-PCRs were performed using the ABI Prism 7700 sequence detection system (Applied Biosystems) using the TaqMan Universal PCR Master Mix (Applied Biosystems) and the universal thermal cycling parameters (2 min at 50°C and 10 min at 95°C, followed by 40 cycles of 15 s at 95°C and 1 min at 60°C). Arbitrary units of target mRNA were corrected by measuring the levels of glyceraldehyde-3-phosphate dehydrogenase mRNA in the paralleled PCR.

The nucleotide sequences of primers and probes are shown in Table 1.

RESULTS

Insulin induces LCFA uptake and FATP1 translocation. To test whether insulin-triggered LCFA uptake by a variety of tissues coincides with the expression of any particular FATP, we compared FATP protein levels to insulin-induced fatty acid uptake rates (Table 2). Data from this experiment were consistent with the hypothesis that FATP1 mediates the insulin-inducible LCFA uptake (Table 2). FATP4 is also expressed in insulin-sensitive tissues (Table 2) but has been shown to be the primary fatty acid transporter in the small intestine (45), a tissue that does not respond to insulin stimulation with increased LCFA uptake (Table 2). In soleus muscle, insulin

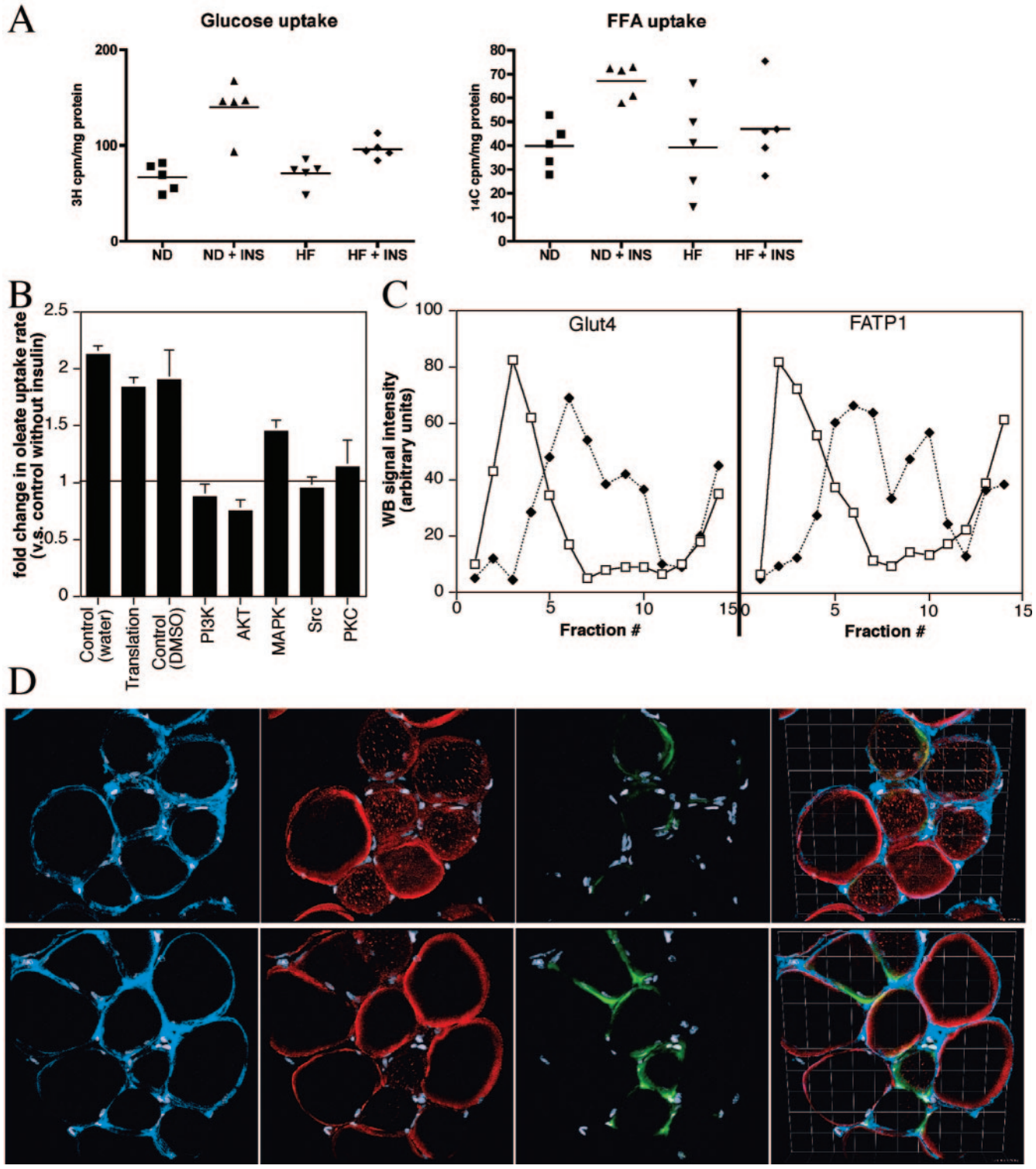

FIG. 1. Insulin-induced translocation of FATP1 in skeletal muscle. (A) Concomitant measurement of 2-deoxy-D-[1-^{3}H]glucose and [^{14}C]oleate uptake into insulin-treated (INS) or untreated soleus muscle from FATP1 wild-type mice fed a normal (ND) or high-fat (HF) diet for 12 weeks. FFA, free fatty acid. (B) Effect of insulin signaling inhibitors on LCFA uptake in 3T3-L1 adipocytes. Serum-starved 3T3-L1 adipocytes were preincubated with inhibitors (at a twofold IC_{50}) of translation (NSC119889, 3 mM), phosphatidylinositol 3-kinase (PI3K; wortmannin; 5 nM), AKT (NSC154020, 20 mM), mitogen-activated protein kinase (MAPK; U0126; 0.1 mM), Src (PP2, 10 nM; note that this compound may also inhibit insulin receptor kinase and PKC with an IC_{50} of 10 μM), or PKC (Go 6850, 0.5 mM) for 30 min followed by a 30-min incubation with 100 nM insulin. NSC119889 was dissolved in water; all other compounds were in dimethyl sulfoxide (DMSO). The 1-minute uptake of [^{14}C]oleate was determined following the insulin incubation. Uptake rates were measured by normalizing ^{14}C counts to protein concentrations and expressed as increase over control uptake in the absence of insulin. Values represent means of six measurements ± standard deviations. (C) Amounts of Glut4

increased both glucose and oleic acid uptake to comparable extents (Fig. 1A). Interestingly, chronic high-fat feeding impaired the insulin response in both transport systems (Fig. 1A), highlighting overlaps in the signaling pathways for glucose and fatty acid transporter translocation. These similarities were also obvious when 3T3-L1 adipocytes were preincubated with inhibitors (at a twofold IC_{50} concentration) of translation (NSC119889, 3 mM [34], phosphatidylinositol 3-kinase [wortmannin, 5 nM] [35], AKT [NSC154020, 20 mM] [57], mitogen-activated protein kinase [U0126, 0.1 mM] [14], Src [PP2, 10 nM] [22] [may also inhibit insulin receptor kinase and protein kinase C {PKC } with an IC_{50} of 10 μM for both {29, 38}], or PKC [Go 6850, 0.5 mM] [26]) (Fig. 1B). Similar results were obtained using respective concentrations of inhibitors at 10-fold their IC_{50}s. Importantly, inhibition of translation did not significantly impact the insulin-induced increase in fatty acid uptake. We have previously shown that insulin causes FATP1 translocation to the plasma membrane and enhanced LCFA uptake in adipocytes (44). To demonstrate that insulin-induced FATP1 translocation is not unique to adipocytes, we used continuous gradient sedimentation of insulin-stimulated and unstimulated skeletal muscle to analyze changes in the subcellular localization of FATP1 and GLUT4. A 30-min insulin stimulus induced a shift of FATP1 to lighter fractions, similar to changes observed for GLUT4 by us (Fig. 1C) and others (7). To visualize FATP1 protein in muscle, we used immunofluorescence microscopy of isolated soleus muscles incubated with or without insulin for 30 min. The sarcolemma was highlighted using an anti-caveolin 3 antibody, and costainings were performed using antibodies against FATP1 (44) and CD36 (16). Three-dimensional reconstruction of surfaces showed a robust sarcolemmal staining and a pronounced intracellular FATP1 vesicle population under insulin-free conditions (Fig. 1D). In contrast, staining of intracellular compartments was greatly reduced in insulin-treated muscle fibers (Fig. 1D). In contrast to FATP1, CD36 was expressed only by a subset of muscle fibers, as had been previously reported (54), and was largely confined to the sarcolemma regardless of insulin treatment.

FATP1 is required for insulin-induced LCFA uptake by adipocytes and muscle. We have previously reported the generation of FATP1-null animals and used hyperinsulinemic-euglycemic clamp studies to show that skeletal muscle of FATP1-knockout mice displays partial protection from lipid infusion-induced insulin resistance and intramuscular accumulation of fatty acyl-CoA (28). However, changes in LCFA uptake in these animals remained undetermined. If FATP1 translocation is indeed causal to the increased LCFA uptake in peripheral insulin-sensitive tissues, one would expect the insulin response in adipocytes and skeletal muscle to be blunted in FATP1-knockout animals. To test this hypothesis, we isolated primary adipocytes and soleus muscle strips from FATP1-null mice and wild-type littermates. Using fluorescent and radiochemical-based LCFA uptake assays, we found that fatty acid uptake in unstimulated adipocytes and soleus muscle was not significantly altered in the absence of FATP1 (Fig. 2A and B). Most importantly, while adipose and muscle tissues from wild-type mice more than doubled their LCFA uptake after a 30-min stimulation with 50 nM insulin, the insulin responsiveness of FATP1-null tissues was greatly blunted (Fig. 2A and B). Insulin-stimulated fatty acid uptake was completely abolished in FATP1-null primary adipocytes (Fig. 2A) and diminished by 80% in soleus muscle (Fig. 2B).

Diminished LCFA uptake by muscle and adipose tissues in vitro also translated into changes in vivo, as the normally rapid drop of serum-free fatty acids after an intraperitoneal insulin injection was significantly delayed, particularly at early time points, in FATP1-null animals (Fig. 2C). Further, oil gavages containing [^{14}C]oleate tracer demonstrated that, while lipid absorption was normal, removal of postprandial lipids was impaired in FATP1-KO mice (Fig. 2D). The delayed removal of postprandial lipids could be indicative of changes in fatty acid biodistribution. In line with this hypothesis, postgavage levels of [^{14}C]oleate tracer in FATP1-KO animals were increased in tissues expressing FATP5, such as liver (24), or FATP6, such as heart (18), but markedly reduced in tissues normally relying on FATP1—most notably white adipose tissue (Fig. 2E) (Table 2).

Adipocytes display significant LCFA fluxes both into and out of cells. Since it was unknown if FATP1 is involved only in the uptake or also in the efflux of fatty acids, we wanted to test whether fatty acid efflux is impaired in FATP1-null adipocytes. To this end, wild-type and FATP1-null primary adipocytes were prepared from epididymal fat pads and stimulated with isobutylmethylxanthine to induce hormone-sensitive lipase activity. Lipolysis of triglycerides produces glycerol besides fatty acids, and glycerol uptake and efflux should be independent of FATP1. Therefore, the ratio between extracellular fatty acids and glycerol should be reduced if fatty acid efflux is impaired but increased if reuptake of fatty acids is affected by loss of FATP1 function. Importantly, this assumption holds true independently of possible changes in the amount of intracellular triglyceride stores, which could have arisen from the formation of fat pads in the absence of FATP1. Figure 2F shows that extracellular LCFA/glycerol ratios are indeed increased in the medium of FATP1-null adipocytes after 1 h of incubation with isobutylmethylxanthine. This strongly argues that FATP1 is predominantly involved in the uptake, but not efflux, of fatty acids. One alternative explanation for the observed data would be that the rate of glycerol phosphorylation, contributing to the glycerol 3-phosphate pool used for reesterification of triglycerides, is increased in FATP1-null adipocytes. However, we have no indication that this is indeed the case. Further, given the strong sequence conservation among the FATP family members (43), it is likely that FATP2 to -6 are also primarily involved in LCFA uptake rather than efflux.

and FATP1 protein in fractions from density gradient centrifugations of soleus muscle lysates were assessed by Western blotting (WB) and densitometry. Open squares, without insulin; closed diamonds, with 50 nM insulin for 30 min. (D) Three-dimensional surface projections of caveolin 3 (blue), FATP1 (red), and CD36 (green), as well as their superimposition (rightmost panels) from 20-μm sections of hind limb muscle from fasted (upper panels) or insulin-injected (lower panels) FATP1 wild-type mice. Nuclei were stained with 4′,6′-diamidino-2-phenylindole and are depicted in turquoise. Grid cell dimensions: 20 by 20 by 20 μm.

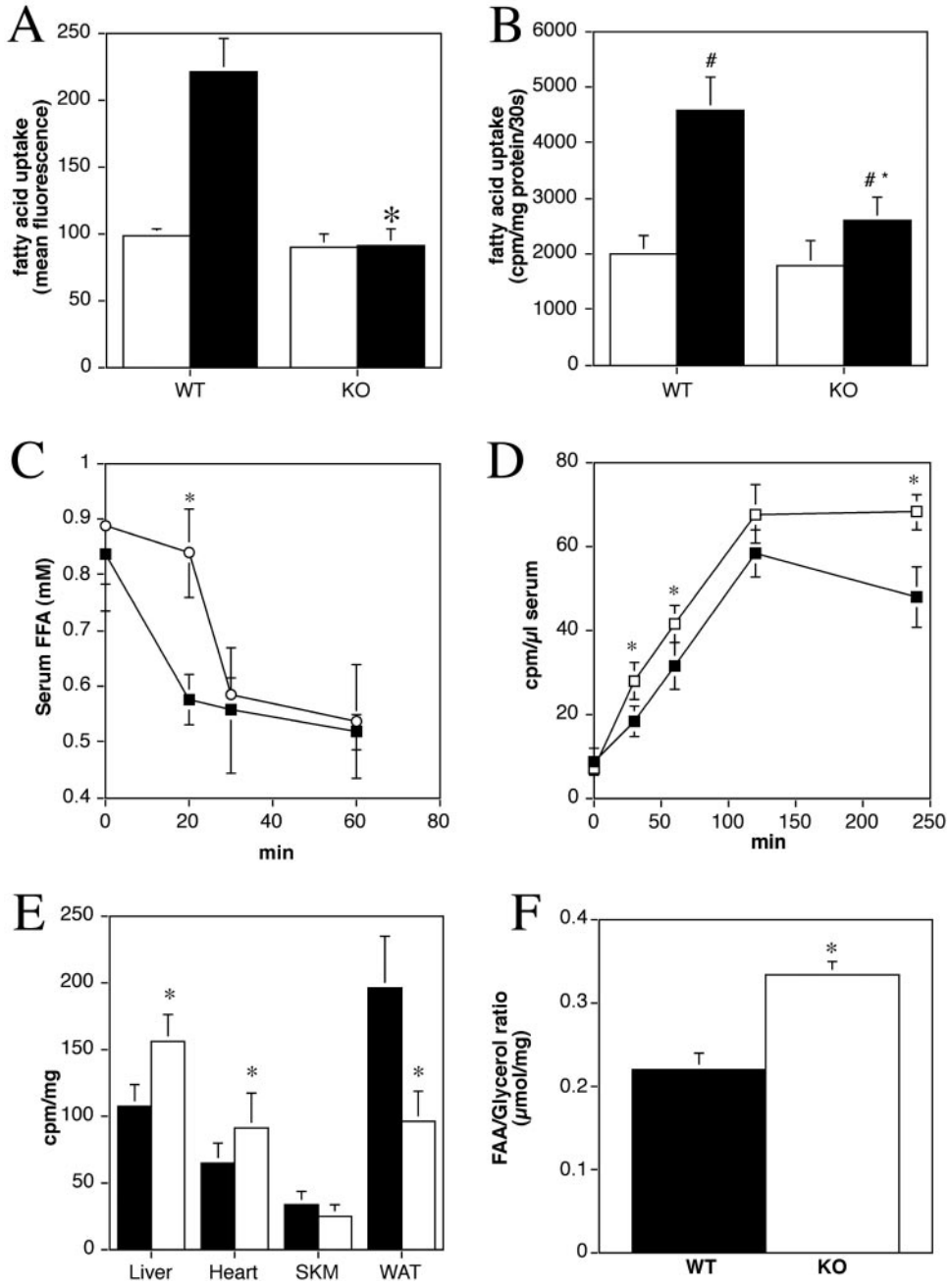

FIG. 2. FATP1-dependent fatty acid flux. (A) Uptake of a fluorescently labeled long-chain fatty acid by primary adipocytes from FATP1 wild-type (WT) and KO animals following a 30-min incubation in RPMI (white bars) or RPMI containing 50 nM insulin (black bars). (B) Rates of uptake of [^{14}C]oleate by soleus muscle strips from FATP1 wild-type and knockout animals following a 30-min incubation in RPMI (white bars) or RPMI containing 50 nM insulin (black bars). (C) Serum free fatty acid (FFA) levels following an intraperitoneal insulin injection in FATP1 wild-type (squares) and knockout (circles) animals. (D) Time course of plasma radioactivity after intragastric administration of 200 μl olive oil containing 2 μCi [^{14}C]oleic acid in FATP1 wild-type (squares) and knockout (open squares) animals. Error bars indicate standard deviations of five mice per group. P was <0.05 at 30 min, 60 min, and 4 h after bolus administration. (E) Distribution of radioactivity in organs of FATP1 wild-type (solid bars) and knockout (open bars) mice 4 h after bolus administration. Error bars indicate standard deviations of five mice per group. SKM, skeletal muscle; WAT, white adipose tissue. (F) Ratios of free fatty acid (FAA) and glycerol efflux from isolated primary FATP1 wild-type and knockout mouse adipocytes. Error bars indicate standard deviations of five measurements. Asterisks and number signs denote a P of <0.05 in Student's t test comparing FATP1 wild-type and KO mice or insulin-treated and untreated mice, respectively.

FATP1-null mice are protected from diet-induced obesity and metabolic syndrome. The delayed insulin-induced clearance of serum fatty acids that we observed could indicate that LCFAs in FATP1-null mice are redirected away from adipose tissue and muscle, possibly towards the liver. This redistribution could potentially alter energy expenditure and susceptibility to diet-induced obesity and diabetes. To test the latter hypothesis, we fed FATP1-null mice and wild-type littermates

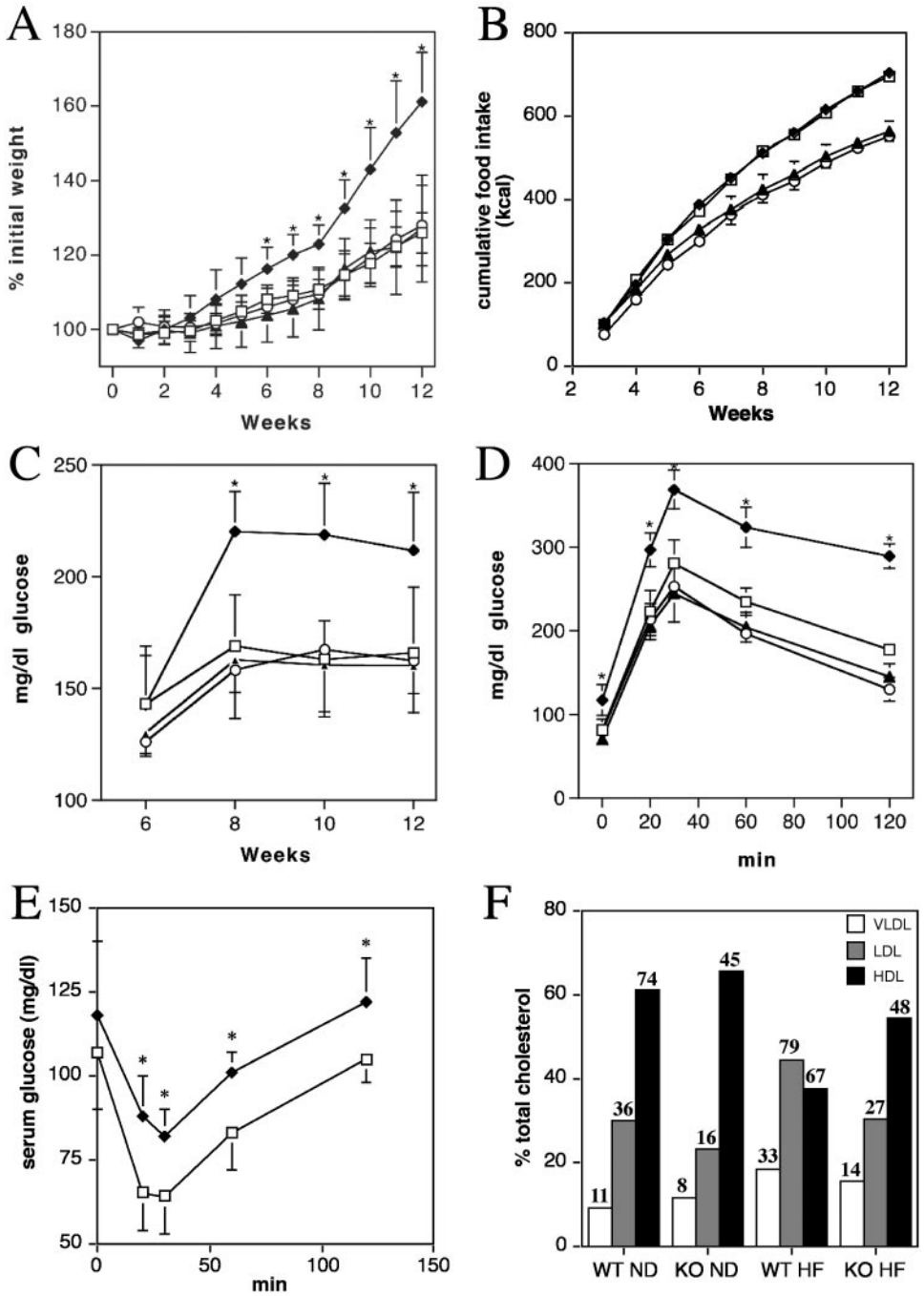

FIG. 3. Diet-induced obesity in wild-type and FATP1-null mice. (A to E) FATP1 wild-type (black symbols) or knockout (white symbols) mice were fed either a low-fat (triangles and circles) or high-fat (diamonds and squares) diet for 12 weeks. Weight gain (A), caloric consumption (B), and serum glucose levels (C) were assessed over the 12-week period. At the end of the study, glucose (D) and insulin (E) tolerance tests were performed. Error bars indicate standard deviations of five measurements. Asterisks denote $P < 0.05$ in Student's t test comparing FATP1 wild-type and KO mice. (F) Lipoprotein profiles of serum pools (four animals each) from wild-type (WT) and FATP1-null (KO) mice fed a normal diet (ND) or a high-fat diet (HF) were generated by FPLC. Bars indicate percentages of total cholesterol in the VLDL (white), LDL (gray), and high-density lipoprotein (HDL; black) peak fractions. Numbers indicate absolute cholesterol levels in mg/dl.

either a low-fat (10% cal from fat) or a high-fat (60% cal from fat, predominantly lard) chow. We repeated studies twice using six male animals per study group. As expected, wild-type mice on the high-fat diet gained significantly more weight than the low-fat chow-fed animals (Fig. 3A). In contrast, FATP1 knockout animals were protected from high-fat diet-induced weight gain and showed no significant difference in weight from either wild-type or knockout animals fed a low-fat chow (Fig. 3A). This was not due to a difference in feeding behavior since caloric consumption in knockout and wild-type animals was

TABLE 3. Serum parameters of FATP1 wild-type and knockout mice[a]

Serum parameter	Value for mouse group:			
	WT ND	WT HF	KO ND	KO HF
Fasting insulin (ng/ml)	0.186 ± 0.046	0.238 ± 0.030	0.200 ± 0.023	**0.192 ± 0.028**
Fed insulin (ng/ml)	0.604 ± 0.100	1.016 ± 0.138	0.470 ± 0.111	**0.560 ± 0.108**
Fasting glucose (mg/dl)	90.4 ± 12.9	97.4 ± 10.5	**77.4 ± 12.1**	**73.8 ± 8.2**
Fed glucose (mg/dl)	176.2 ± 13.5	238.8 ± 28.5	**142.6 ± 16.5**	**147.2 ± 13.7**
Fasting TG (mg/dl)	63.4 ± 6.3	78.6 ± 12.1	54.8 ± 8.5	**55.8 ± 16.7**
Fed TG (mg/dl)	166.8 ± 20.7	239.4 ± 15.5	**131.0 ± 12.6**	**134.0 ± 23.6**
Fasting FFA (mM)	2.2 ± 0.1	2.4 ± 0.1	**2.0 ± 0.2**	**2.0 ± 0.1**
Fed FFA (mM)	1.4 ± 0.1	1.5 ± 0.2	**1.1 ± 0.1**	**1.2 ± 0.2**

[a] Fasting and fed serum levels of insulin, glucose, TGs, and free fatty acids (FFA) in FATP1 wild-type (WT) and KO animals fed a low-fat (ND) or high-fat (HF) chow for 12 weeks. The standard deviation of at least five measurements is given. Boldface values indicate a P of <0.05 in Student's t test comparing FATP wild-type and KO animal values.

identical (Fig. 3B). Glucose levels, measured by tail bleeds in ad libitum-fed animals, started to rise after 8 weeks in the high-fat diet/wild-type group, indicating a loss of glycemic control. In contrast, glucose levels in the FATP1-null high-fat group remained normal (Fig. 3C). In line with these observations, the glucose tolerance test (Fig. 3D) and the insulin tolerance test (Fig. 3E), performed at the end of the 12-week feeding study, showed impaired insulin sensing in high-fat-fed wild-type but not FATP1-knockout animals. At this time point, we also determined fasting and fed serum values for insulin, glucose, triglycerides, and free fatty acids (Table 3). While the high-fat-fed wild-type animals had developed a pattern consistent with the onset of metabolic syndrome, FATP1-null animals were completely protected from these alterations (Table 3). This was also evident from the analysis of lipoprotein profiles (Fig. 3F) that showed for wild-type, but not FATP1-null, animals a conversion to a high-LDL/proatherosclerotic profile following high-fat feeding (Fig. 3F). Additionally, profiling of serum adipokines showed significantly lower leptin and resistin levels in FATP1-null mice fed a high-fat diet, while adiponectin levels were higher than those in wild-type littermates (Table 4).

Triglyceride and morphometric analysis of organs at the end of the feeding studies further supported the notion that chronic loss of FATP1 function leads to a redistribution of lipids among organs. Liver weights and triglyceride contents of FATP1-knockout animals were significantly increased in both high- and low-fat-fed animals (Fig. 4A and B), and mice displayed pronounced lipid droplet accumulation on the high-fat diet (Fig. 4C). Interestingly, β-oxidation rates in liver slices from FATP1 animals were clearly elevated (Fig. 4D)—possibly reflecting a fatty acid-induced activation of peroxisome proliferator-activated receptor α (PPAR-α) (30). While real-time PCR analysis of mRNA levels revealed similar expression of PPAR-α in livers of knockout and wild-type animals fed a high-fat diet, several PPAR-α target genes such as FABP1, CPT1, and UCP2 were strongly up regulated in the livers of FATP1-null mice (Table 5). Interestingly, expression of liver fatty acid transporters FATP2, FATP5, and CD36 revealed a small but significant up regulation of these transporters in the FATP1-knockout mice (Table 5).

Significantly, epididymal fat pads from FATP1-null animals were considerably smaller not only in the overall lighter high-fat group but also in the normal chow cohort (Fig. 5C). Interestingly, fat pad differences were primarily due to a significant reduction in adipocyte size (Fig. 5A and B) rather than a reduced cell number. Further, muscle triglyceride content was also reduced in both the basal and chronic high-fat groups (Fig. 5D). However, differences in muscle TG content did not affect motor strength (data not shown).

TABLE 4. Serum adipokine levels of FATP1 wild-type and knockout mice[a]

Adipokine	Value for mouse group:			
	WT ND	WT HF	KO ND	KO HF
Adiponectin (μg/ml)	14.6 ± 0.3	12.8 ± 1.3	**15.4 ± 0.6**	**14.9 ± 1.4**
Resistin (ng/ml)	25.2 ± 1.5	35.5 ± 6.3	22 ± 3.6	**25.9 ± 3**
Leptin (ng/ml)	8 ± 0.7	11 ± 2	6.5 ± 1.6	**7.1 ± 1.8**

[a] Fasting serum levels of adiponectin, resistin, and leptin from FATP1 wild-type (WT) and knockout animals fed a low-fat (ND) or high-fat (HF) chow for 12 weeks. The standard deviation of at least five measurements is given. Boldface values indicate a P of <0.05 in Student's t test comparing FATP1 wild-type and KO animal values.

DISCUSSION

Insulin plays an important role in maintaining nutrient homeostasis. Postprandial surges of insulin reduce serum glucose both by decreasing hepatic glucose output and by increasing glucose uptake. The latter is primarily due to increased activity of the glucose transporter GLUT4 in muscle and adipose tissue (13). Regulation of serum LCFA levels is equally important particularly since chronically elevated serum fatty acid levels have been linked to the development of insulin desensitization (6, 41). While it is known that insulin suppresses the release of LCFAs from white adipose tissue by inhibiting hormone-sensitive lipase (25), it has remained unclear if LCFA uptake is also a regulated process. Here we took advantage of a genetic model system that lacks the LCFA transporter FATP1 to demonstrate that, analogous to the regulation of glucose, LCFA uptake is also dynamically regulated by insulin. Loss of FATP1 practically abolished insulin-induced LCFA uptake in adipocytes and skeletal muscle and led to a redistribution of dietary lipids away from fat and skeletal muscle and towards the liver. Likely as a consequence of this redistribution, FATP1-null animals are protected from the insulin-desensitizing effects of a high-fat diet.

FATP1's expression pattern is consistent with its proposed

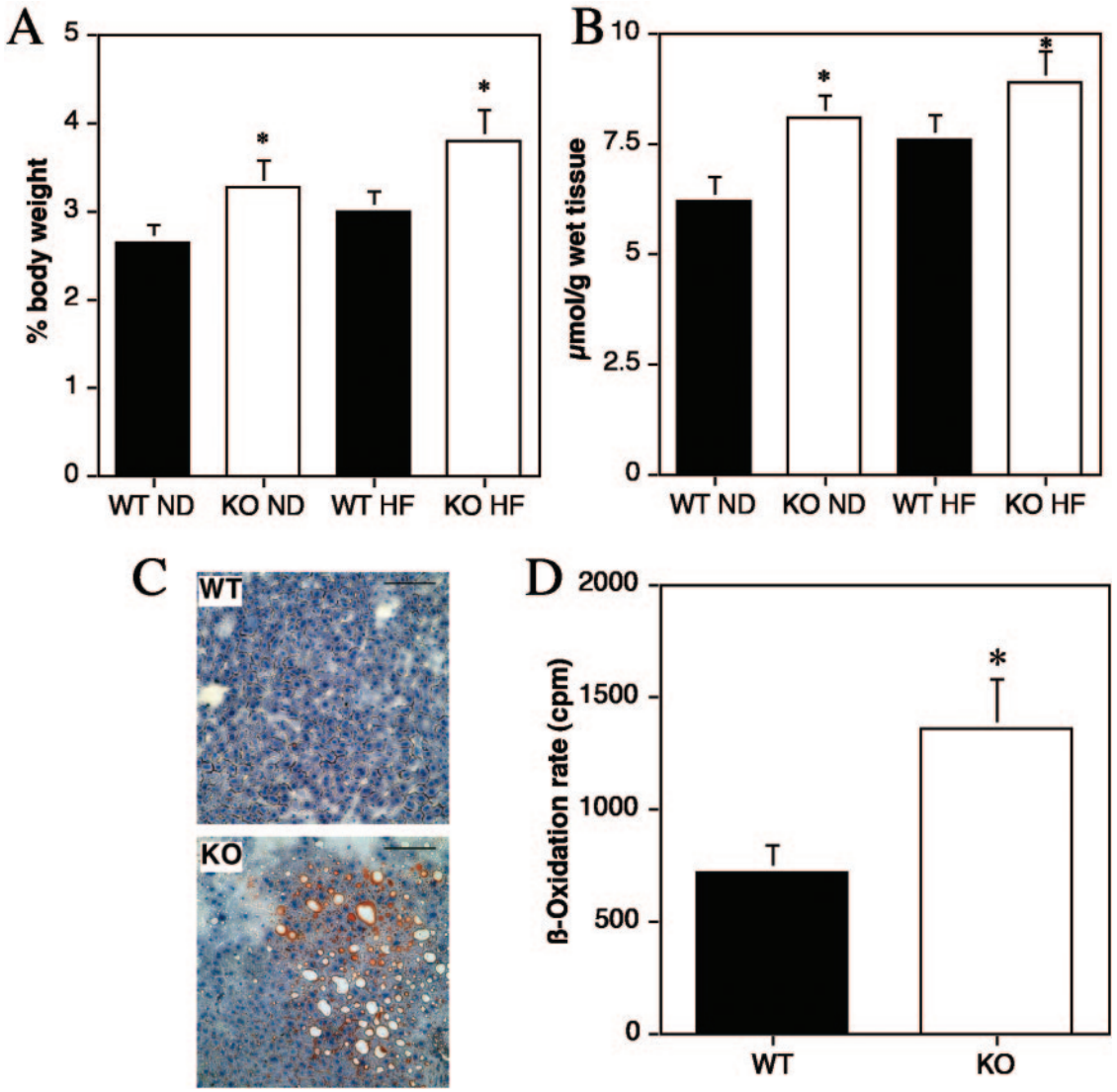

FIG. 4. Changes in FATP1-null mouse livers. (A) Liver weight relative to body mass. (B) Extractable liver triglycerides normalized to g (wet weight). (C) Oil red O staining of wild-type and FATP1-null mouse livers from mice fed a high-fat diet for 12 weeks. Bars: 100 μm. (D) β-Oxidation assay with liver slices from male FATP1 wild-type and null (KO) animals. Error bars indicate standard deviations of at least five measurements. Asterisks denote a P of <0.05 in Student's t test comparing FATP1 wild-type and KO mice. WT, wild type; ND, low-fat diet; HF, high-fat diet.

role as an insulin-sensitive LCFA transporter since it is abundantly expressed by the two tissues with the largest LCFA uptake response to insulin, white adipose tissue and skeletal muscle, but is absent from other insulin-sensitive tissues that lack the insulin-induced LCFA uptake, such as the liver. Interestingly, we show here that high-fat-induced insulin desensitization impairs both insulin-stimulated glucose and LCFA uptake (Fig. 1A), arguing that the two signaling pathways overlap significantly. This is a notion that is further supported by our preliminary analysis of insulin signaling pathways leading to FATP1 translocation and increased LCFA uptake (Fig. 1B). It seems perplexing that insulin-inducible LCFA uptake is blunted in mice after a high-fat diet treatment. Yet FATP1-KO mice are protected from diet-induced obesity and insulin resistance. However, the two observations can be reconciled when assuming that FATP1-mediated LCFA uptake is particularly important for insulin desensitization during the early phase of diet-induced obesity, which is characterized by hyperinsulinemia. We hypothesize that during this prediabetic phase the increased insulin leads to a predominantly FATP1-mediated accumulation of lipids in muscle which in turn leads to insulin desensitization and hyperglycemia. However, FATP1-mediated uptake may be less important once an overtly diabetic phenotype has been established.

As a mechanism for the insulin-induced LCFA uptake, we propose a translocation of FATP1 from an intracellular compartment to the plasma membrane. While this process has been observed for adipocytes (44) as well as skeletal muscle (Fig. 1C and D), we cannot exclude additional activation mechanisms such as covalent modification of FATP1 or accessory molecules. However, the fact that loss of FATP1 greatly diminishes insulin-induced LCFA uptake strongly argues that it

TABLE 5. Changes in liver expression[a]

Diet and gene	Trend[b]	mRNA abundance in mouse group:				*P*
		WT		KO		
		Avg	SD	Avg	SD	
Normal diet						
FATP2	↑	3.64	0.11	5.4	0.17	0.00024
FATP5	↑	18	1.44	20.6	2.79	0.062
CD36	↔	10.7	1.56	10.1	2.98	0.18
FABP1	⇑	93.1	2.80	246.7	7.63	0.00001
CPT1	↑	7.9	0.82	11.2	0.97	0.00997
UCP2	↓	2.3	1.05	1.0	0.10	0.01114
SREBP-1c	↓	28.0	2.42	17.9	2.80	0.00889
PPAR-α	↓	2.8	0.42	1.1	0.13	0.00151
PGC-1	↔	9.1	0.61	10.1	0.65	0.12495
High-fat diet						
FATP2	↓	5.4	0.13	2.0	0.12	0.00014
FATP5	↑	22.4	4.76	29.1	7.27	0.00492
CD36	↑	32.5	3.59	39.4	2.01	0.0062
FABP1	⇑	383.8	18.7	963.2	32.8	0.00001
CPT1	⇑	15.1	0.82	68.5	4.43	0.00003
UCP2	⇑	9.8	1.71	34.3	7.05	0.00413
SREBP-1c	⇓	45.3	1.53	16.3	0.46	0.00001
PPAR-α	↓	15.8	1.84	10.4	1.87	0.02273
PGC-1	↑	7.6	0.32	10.7	0.31	0.00024

[a] mRNA abundance of the indicated genes (in arbitrary units) was determined by real-time PCR and normalized to glyceraldehyde-3-phosphate dehydrogenase expression. mRNAs from five mice per group were pooled and assayed independently three times. Averages, standard deviations, and significances based on the unpaired Student *t* test are shown.

[b] Symbols: ↑, upward; ↓, downward; ↔, no change; ⇑, strongly upward; ⇓, strongly downward.

is required for this process. In the same tissues, we failed to observe a translocation of other proteins involved in LCFA uptake such as FATP4 and CD36, albeit a change of CD36 subcellular localization in response to insulin was observed by others using membrane fractionation techniques (32). Indeed, the small but significant ($P = 0.003$) remaining FATP1-independent insulin response in muscle hints at additional mechanisms relying on other plasma membrane proteins, e.g., FATP4 (43) and CD36 (11), or may reflect changes in intracellular lipid metabolism. Basal LCFA uptake by adipocytes and skeletal muscle, in contrast, was not significantly impaired, leading us to hypothesize that basal uptake in the absence of insulin is predominantly mediated by other proteins or mechanisms. Possible candidate genes that might mediate the basal uptake include FATP4 (17, 45) and CD36 (2). The contribution of FATP4 to LCFA uptake in muscle or adipocytes has not yet been tested since FATP4 animals are embryonic lethal (17), but antisense-mediated down regulation of FATP4 in primary enterocytes led to a robust reduction in LCFA uptake rates (45). CD36 has been shown to be required for efficient uptake of oleate by adipocytes at low fatty-acid-to-BSA ratios (15). Importantly, the complete lack of insulin-stimulated LCFA uptake by FATP1-null adipocytes and the greatly reduced LCFA uptake by skeletal muscle in response to insulin show that FATP1 is crucially required for insulin's effect on LCFA uptake independently of other insulin actions such as increased glucose uptake. Taken together, these data demonstrate for the first time that dynamic regulation of fatty acid uptake by peripheral tissues depends on an insulin-sensitive FATP1 compartment. The concept of insulin-stimulated LCFA uptake is functionally analogous to the Glut4 compartment, and it will be interesting to study the overlap of the two transporter populations in the future.

The importance of the insulin-induced LCFA uptake system is highlighted by the decreased serum LCFA absorption rate and the change of dietary lipid deposition away from FATP1 expression organs, i.e., fat and skeletal muscle, towards organs whose LCFA uptake is dominated by other FATP family members such as the liver, expressing FATP5 and -2 (24), as well as the heart, which primarily expresses FATP6 (18). While loss of FATP1 function led to a pronounced redistribution of lipids, it is worth noting that it is not the only protein that can become rate limiting for LCFA uptake. Lipoprotein lipase (LpL) is the principal enzyme that generates fatty acids in the extrahepatic circulation through the hydrolysis of chylomicrons and VLDL particles. Through tissue-specific gain (23, 27, 31, 56)- and loss (4)-of-function studies, it has been demonstrated that local activity of LpL can control the rate of lipid accumulation and, in the case of muscle-specific overexpression, can lead to insulin desensitization (27).

Likely as a result of the observed lipid redistribution, loss of FATP1 conferred a strong resistance to high-fat diet-induced obesity, insulin desensitization, and the onset of metabolic syndrome (Fig. 3). Increased adiposity, particularly visceral obesity (33), as well as increased muscle triglyceride content (41), has been linked to the development of the metabolic syndrome. Using hyperinsulinemic-euglycemic clamp studies following lipid injections or short-term high-fat challenges (28), we have previously shown that muscle from FATP1-knockout mice is partially protected from insulin signaling. Here we report that, following high-fat feeding, adipocyte mass and cell size, which frequently correlate with insulin sensitivity (55), are also reduced. Increased insulin sensitivity can also be inferred from the improved adipokine profiles in FATP1-null mice fed a high-fat diet, which demonstrated reduced leptin and resistin levels and increased serum concentrations of adiponectin. Since loss of FATP1 function affects both fat and muscle, dual mechanisms might underlie the observed resistance to diet-induced obesity and diabetes. Further studies using the tissue-specific reexpression of FATP1 in the background of FATP1-null mice are under way to address these interesting questions. These findings are in contrast to CD36-null mice, which also have decreased muscle TG content (20) and decreased rates of LCFA uptake into adipocytes (15) but are not protected from a high-fat diet (safflower)-induced insulin desensitization (20) and have increased resting cholesterol, TG, and LCFA levels (15).

Since FATP1-null mice consume equal amounts of calories as do their wild-type littermates on a high-fat diet but resist obesity, the question of the fate of the excess energy arises. We found that fatty acids in FATP1-null animals are shunted into the liver, which is enlarged and TG enriched in these animals and, importantly, shows an increased rate of oleate β-oxidation. Fatty acid transporters FATP2, FATP5, and CD36 were only slightly up regulated in FATP1-null mouse livers (Table 5), arguing that increased LCFA uptake was mainly driven by the increased and prolonged postprandial levels of dietary lipids. Further, livers from FATP1-null animals fed a high-fat diet express significantly higher levels of FABP1 (2.5-fold increase),

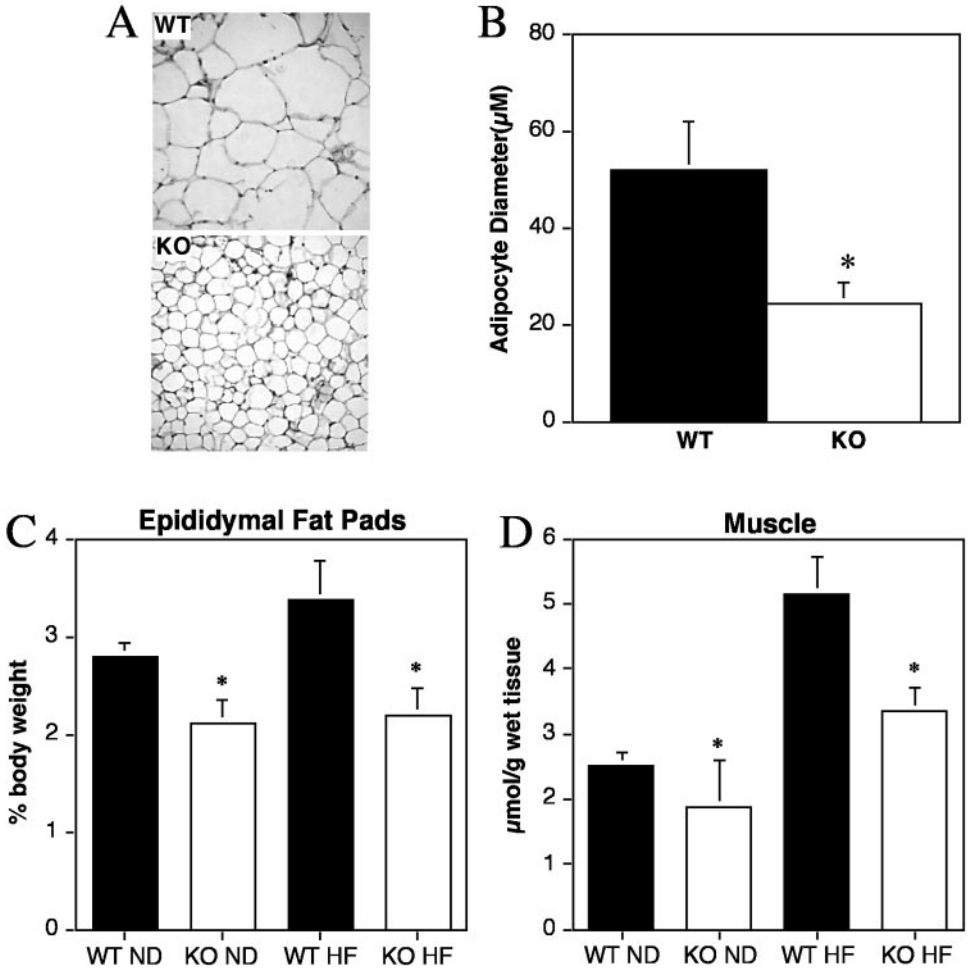

FIG. 5. Phenotypic changes in FATP1-null animals. (A) Hematoxylin- and eosin-stained white adipose tissue sections of wild-type and FATP1 knockout mice. (B) Average adipocyte diameter determined from fat pad sections as shown in panel A. (C) Epididymal fat pad weights relative to body mass. (D) Muscle TG content. ND, low-fat diet; HF, high-fat diet; WT, wild type; black bars, wild-type mice; white bars, FATP1-null animals. Error bars indicate standard deviations of at least five measurements. Asterisks denote a P of <0.05 in Student's t test comparing FATP1 wild-type and KO mice.

CPT1 (4.6-fold increase), and UCP2 (3.5-fold increase), in line with increased lipid handling and oxidation capacity (Table 5). Interestingly, all three genes are regulated in the liver by PPAR-α, indicating that, while overall PPARα levels were lower or unchanged (Table 5), PPAR-α activity was increased, possibly due to the increased availability of natural ligands such as fatty acids and their acyl-CoA esters (30).

Taken together, these findings demonstrate for the first time in vivo that a system analogous to the insulin-sensitive glucose transporter GLUT4 exists for fatty acids. We propose a model in which insulin counteracts the postprandial rise in dietary lipids by increasing active FATP1, primarily in adipocytes and skeletal muscle, while basal LCFA uptake by these and other tissues is mediated by other FATPs in conjunction with CD36. In the absence of FATP1, dietary fatty acid uptake by adipocytes and skeletal muscle is reduced, protecting them from insulin desensitization, while uptake by liver is increased. This is potentially activating PPAR-α and triggering increased β-oxidation by this organ (30), thus preventing the detrimental effects of a high-fat diet that otherwise might have led to the onset of hepatic steatosis and insulin resistance. Therefore, we argue that FATP1 plays an important role in the removal of postprandial fatty acids by adipose tissue and muscle as well as in the etiology of diet-induced insulin resistance and metabolic disease. This highlights the role of protein-mediated fatty acid uptake versus a simple unregulated mechanism based on diffusion as previously proposed (21). Consequently, inhibitors of FATP1 function might be useful as novel therapeutic approaches for the treatment of insulin resistance, type 2 diabetes, and cardiovascular disease.

ACKNOWLEDGMENTS

We thank M. Febbraio for providing the CD36 antibody, the staffs of the Stanford Imaging Center and the PAMFRI animal facility for their support and advice, and R. Grammer for her help in preparing the manuscript.

This work was supported by grants to A.S. from the National Institutes of Health, NIDDK (NIH DK066336-01), and a Career Development Award from the American Diabetes Association.

REFERENCES

1. **Abel, E. D., O. Peroni, J. K. Kim, Y. B. Kim, O. Boss, E. Hadro, T. Minnemann, G. I. Shulman, and B. B. Kahn.** 2001. Adipose-selective targeting of the GLUT4 gene impairs insulin action in muscle and liver. Nature **409:**729–733.
2. **Abumrad, N., C. Coburn, and A. Ibrahimi.** 1999. Membrane proteins implicated in long-chain fatty acid uptake by mammalian cells: CD36, FATP and FABPm. Biochim. Biophys. Acta **1441:**4–13.
3. **Abumrad, N., C. Harmon, and A. Ibrahimi.** 1998. Membrane transport of long-chain fatty acids: evidence for a facilitated process. J. Lipid Res. **39:**2309–2318.
4. **Augustus, A., H. Yagyu, G. Haemmerle, A. Bensadoun, R. K. Vikramadithyan, S. Y. Park, J. K. Kim, R. Zechner, and I. J. Goldberg.** 2004. Cardiac-specific knock-out of lipoprotein lipase alters plasma lipoprotein triglyceride metabolism and cardiac gene expression. J. Biol. Chem. **279:**25050–25057.
5. **Binnert, C., H. A. Koistinen, G. Martin, F. Andreelli, P. Ebeling, V. A. Koivisto, M. Laville, J. Auwerx, and H. Vidal.** 2000. Fatty acid transport protein-1 mRNA expression in skeletal muscle and in adipose tissue in humans. Am. J. Physiol. Endocrinol. Metab. **279:**E1072–E1079.
6. **Boden, G.** 1997. Role of fatty acids in the pathogenesis of insulin resistance and NIDDM. Diabetes **46:**3–10.
7. **Bonen, A., J. Luiken, Y. Arumugam, J. Glatz, and N. Tandon.** 2000. Acute regulation of fatty acid uptake involves the cellular redistribution of fatty acid translocase. J. Biol. Chem. **275:**14501–14508.
8. **Carley, A. N., L. M. Semeniuk, Y. Shimoni, E. Aasum, T. S. Larsen, J. P. Berger, and D. L. Severson.** 2004. Treatment of type 2 diabetic db/db mice with a novel PPARγ agonist improves cardiac metabolism but not contractile function. Am. J. Physiol. Endocrinol. Metab. **286:**E449–E455.
9. **Chiu, H. C., A. Kovacs, D. A. Ford, F. F. Hsu, R. Garcia, P. Herrero, J. E. Saffitz, and J. E. Schaffer.** 2001. A novel mouse model of lipotoxic cardiomyopathy. J. Clin. Investig. **107:**813–822.
10. **Coburn, C. T., T. Hajri, A. Ibrahimi, and N. A. Abumrad.** 2001. Role of CD36 in membrane transport and utilization of long-chain fatty acids by different tissues. J. Mol. Neurosci. **16:**117–121.
11. **Coburn, C. T., F. F. Knapp, Jr., M. Febbraio, A. L. Beets, R. L. Silverstein, and N. A. Abumrad.** 2000. Defective uptake and utilization of long chain fatty acids in muscle and adipose tissues of CD36 knockout mice. J. Biol. Chem. **275:**32523–32529.
12. **Coe, N., A. Smith, B. Frohnert, P. Watkins, and D. Bernlohr.** 1999. The fatty acid transport protein (FATP1) is a very long chain acyl-CoA synthetase. J. Biol. Chem. **274:**36300–36304.
13. **Cushman, S. W., L. J. Goodyear, P. F. Pilch, E. Ralston, H. Galbo, T. Ploug, S. Kristiansen, and A. Klip.** 1998. Molecular mechanisms involved in GLUT4 translocation in muscle during insulin and contraction stimulation. Adv. Exp. Med. Biol. **441:**63–71.
14. **Duncia, J. V., J. B. Santella III, C. A. Higley, W. J. Pitts, J. Wityak, W. E. Frietze, F. W. Rankin, J. H. Sun, R. A. Earl, A. C. Tabaka, C. A. Teleha, K. F. Blom, M. F. Favata, E. J. Manos, A. J. Daulerio, D. A. Stradley, K. Horiuchi, R. A. Copeland, P. A. Scherle, J. M. Trzaskos, R. L. Magolda, G. L. Trainor, R. R. Wexler, F. W. Hobbs, and R. E. Olson.** 1998. MEK inhibitors: the chemistry and biological activity of U0126, its analogs, and cyclization products. Bioorg. Med. Chem. Lett. **8:**2839–2844.
15. **Febbraio, M., N. A. Abumrad, D. P. Hajjar, K. Sharma, W. Cheng, S. F. Pearce, and R. L. Silverstein.** 1999. A null mutation in murine CD36 reveals an important role in fatty acid and lipoprotein metabolism. J. Biol. Chem. **274:**19055–19062.
16. **Febbraio, M., D. P. Hajjar, and R. L. Silverstein.** 2001. CD36: a class B scavenger receptor involved in angiogenesis, atherosclerosis, inflammation, and lipid metabolism. J. Clin. Investig. **108:**785–791.
17. **Gimeno, R. E., D. J. Hirsch, S. Punreddy, Y. Sun, A. M. Ortegon, H. Wu, T. Daniels, A. Stricker-Krongrad, H. F. Lodish, and A. Stahl.** 2003. Targeted deletion of fatty acid transport protein-4 results in early embryonic lethality. J. Biol. Chem. **278:**49512–49516.
18. **Gimeno, R. E., A. M. Ortegon, S. Patel, S. Punreddy, P. Ge, Y. Sun, H. F. Lodish, and A. Stahl.** 2003. Characterization of a heart-specific fatty acid transport protein. J. Biol. Chem. **278:**16039–16044.
19. **Gore, J., and C. Hoinard.** 1993. Linolenic acid transport in hamster intestinal cells is carrier-mediated. J. Nutr. **123:**66–73.
20. **Hajri, T., X. X. Han, A. Bonen, and N. A. Abumrad.** 2002. Defective fatty acid uptake modulates insulin responsiveness and metabolic responses to diet in CD36-null mice. J. Clin. Investig. **109:**1381–1389.
21. **Hamilton, J. A.** 1999. Transport of fatty acids across membranes by the diffusion process. Prostaglandins Leukot. Essent. Fatty Acids **60:**291–297.
22. **Hanke, J. H., J. P. Gardner, R. L. Dow, P. S. Changelian, W. H. Brissette, E. J. Weringer, B. A. Pollok, and P. A. Connelly.** 1996. Discovery of a novel, potent, and Src family-selective tyrosine kinase inhibitor. Study of Lck- and FynT-dependent T cell activation. J. Biol. Chem. **271:**695–701.
23. **Hensley, L. L., G. Ranganathan, E. M. Wagner, B. D. Wells, J. C. Daniel, D. Vu, C. F. Semenkovich, R. Zechner, and P. A. Kern.** 2003. Transgenic mice expressing lipoprotein lipase in adipose tissue. Absence of the proximal 3′-untranslated region causes translational upregulation. J. Biol. Chem. **278:**32702–32709.
24. **Hirsch, D., A. Stahl, and H. F. Lodish.** 1998. A family of fatty acid transporters conserved from mycobacterium to man. Proc. Natl. Acad. Sci. USA **95:**8625–8629.
25. **Holm, C., T. Osterlund, H. Laurell, and J. A. Contreras.** 2000. Molecular mechanisms regulating hormone-sensitive lipase and lipolysis. Annu. Rev. Nutr. **20:**365–393.
26. **Jacobson, P. B., S. L. Kuchera, A. Metz, C. Schachtele, K. Imre, and D. J. Schrier.** 1995. Anti-inflammatory properties of Go 6850: a selective inhibitor of protein kinase C. J. Pharmacol. Exp. Ther. **275:**995–1002.
27. **Kim, J. K., J. J. Fillmore, Y. Chen, C. Yu, I. K. Moore, M. Pypaert, E. P. Lutz, Y. Kako, W. Velez-Carrasco, I. J. Goldberg, J. L. Breslow, and G. I. Shulman.** 2001. Tissue-specific overexpression of lipoprotein lipase causes tissue-specific insulin resistance. Proc. Natl. Acad. Sci. USA **98:**7522–7527.
28. **Kim, J. K., R. E. Gimeno, T. Higashimori, H. J. Kim, H. Choi, S. Punreddy, R. L. Mozell, G. Tan, A. Stricker-Krongrad, D. J. Hirsch, J. J. Fillmore, Z. X. Liu, J. Dong, G. Cline, A. Stahl, H. F. Lodish, and G. I. Shulman.** 2004. Inactivation of fatty acid transport protein 1 prevents fat-induced insulin resistance in skeletal muscle. J. Clin. Investig. **113:**756–763.
29. **Lawrence, D. S., and J. Niu.** 1998. Protein kinase inhibitors: the tyrosine-specific protein kinases. Pharmacol. Ther. **77:**81–114.
30. **Lee, C. H., P. Olson, and R. M. Evans.** 2003. Minireview: lipid metabolism, metabolic diseases, and peroxisome proliferator-activated receptors. Endocrinology **144:**2201–2207.
31. **Levak-Frank, S., H. Radner, A. Walsh, R. Stollberger, G. Knipping, G. Hoefler, W. Sattler, P. H. Weinstock, J. L. Breslow, and R. Zechner.** 1995. Muscle-specific overexpression of lipoprotein lipase causes a severe myopathy characterized by proliferation of mitochondria and peroxisomes in transgenic mice. J. Clin. Investig. **96:**976–986.
32. **Luiken, J. J., D. J. Dyck, X. X. Han, N. N. Tandon, Y. Arumugam, J. F. Glatz, and A. Bonen.** 2002. Insulin induces the translocation of the fatty acid transporter FAT/CD36 to the plasma membrane. Am. J. Physiol. Endocrinol. Metab. **282:**E491–E495.
33. **Masuzaki, H., J. Paterson, H. Shinyama, N. M. Morton, J. J. Mullins, J. R. Seckl, and J. S. Flier.** 2001. A transgenic model of visceral obesity and the metabolic syndrome. Science **294:**2166–2170.
34. **Novac, O., A. S. Guenier, and J. Pelletier.** 2004. Inhibitors of protein synthesis identified by a high throughput multiplexed translation screen. Nucleic Acids Res. **32:**902–915.
35. **Powis, G., R. Bonjouklian, M. M. Berggren, A. Gallegos, R. Abraham, C. Ashendel, L. Zalkow, W. F. Matter, J. Dodge, G. Grindey, et al.** 1994. Wortmannin, a potent and selective inhibitor of phosphatidylinositol-3-kinase. Cancer Res. **54:**2419–2423.
36. **Reaven, G. M., C. Hollenbeck, C. Y. Jeng, M. S. Wu, and Y. D. Chen.** 1988. Measurement of plasma glucose, free fatty acid, lactate, and insulin for 24 h in patients with NIDDM. Diabetes **37:**1020–1024.
37. **Richieri, G. V., and A. M. Kleinfeld.** 1995. Unbound free fatty acid levels in human serum. J. Lipid Res. **36:**229–240.
38. **Rosenzweig, T., S. Aga-Mizrachi, A. Bak, and S. R. Sampson.** 2004. Src tyrosine kinase regulates insulin-induced activation of protein kinase C (PKC) delta in skeletal muscle. Cell. Signal. **16:**1299–1308.
39. **Schaffer, J. E., and H. F. Lodish.** 1994. Expression cloning and characterization of a novel adipocyte long chain fatty acid transport protein. Cell **79:**427–436.
40. **Schmitz-Peiffer, C.** 2000. Signalling aspects of insulin resistance in skeletal muscle: mechanisms induced by lipid oversupply. Cell. Signal. **12:**583–594.
41. **Shulman, G. I.** 2000. Cellular mechanisms of insulin resistance. J. Clin. Investig. **106:**171–176.
42. **Sorrentino, D., D. Stump, B. J. Potter, R. B. Robinson, R. White, C. L. Kiang, and P. D. Berk.** 1988. Oleate uptake by cardiac myocytes is carrier mediated and involves a 40-kD plasma membrane fatty acid binding protein similar to that in liver, adipose tissue, and gut. J. Clin. Investig. **82:**928–935.
43. **Stahl, A.** 2004. A current review of fatty acid transport proteins (SLC27). Pflugers Arch. **447:**722–727.
44. **Stahl, A., J. G. Evans, S. Pattel, D. Hirsch, and H. F. Lodish.** 2002. Insulin causes fatty acid transport protein translocation and enhanced fatty acid uptake in adipocytes. Dev. Cell **2:**477–488.
45. **Stahl, A., D. J. Hirsch, R. Gimeno, S. Punreddy, P. Ge, N. Watson, M. Kotler, L. A. Tartaglia, and H. F. Lodish.** 1999. Identification of a small intestinal fatty acid transport protein. Mol. Cell **4:**299–308.
46. **Steiner, G., S. Morita, and M. Vranic.** 1980. Resistance to insulin but not to glucagon in lean human hypertriglyceridemics. Diabetes **29:**899–905.
47. **Steneberg, P., N. Rubins, R. Bartoov-Shifman, M. D. Walker, and H. Edlund.** 2005. The FFA receptor GPR40 links hyperinsulinemia, hepatic steatosis, and impaired glucose homeostasis in mouse. Cell Metab. **1:**245–258.
48. **Stiles, B., Y. Wang, A. Stahl, S. Bassilian, W. P. Lee, Y. J. Kim, R. Sherwin, S. Devaskar, R. Lesche, M. A. Magnuson, and H. Wu.** 2004. Live-specific deletion of negative regulator Pten results in fatty liver and insulin hypersensitivity. Proc. Natl. Acad. Sci. USA **101:**2082–2087.
49. **Stremmel, W.** 1989. Mechanism of hepatic fatty acid uptake. J. Hepatol. **9:**374–382.

50. **Stremmel, W.** 1989. Transmembrane transport of fatty acids in the heart. Mol. Cell. Biochem. **88:**23–29.
51. **Stremmel, W.** 1988. Uptake of fatty acids by jejunal mucosal cells is mediated by a fatty acid binding membrane protein. J. Clin. Investig. **82:**2001–2010.
52. **Stump, D. D., X. Fan, and P. D. Berk.** 2001. Oleic acid uptake and binding by rat adipocytes define dual pathways for cellular fatty acid uptake. J. Lipid Res. **42:**509–520.
53. **Tremblay, F., M. J. Dubois, and A. Marette.** 2003. Regulation of GLUT4 traffic and function by insulin and contraction in skeletal muscle. Front. Biosci. **8:**d1072–d1084.
54. **Vistisen, B., K. Roepstorff, C. Roepstorff, A. Bonen, B. van Deurs, and B. Kiens.** 2004. Sarcolemmal FAT/CD36 in human skeletal muscle colocalizes with caveolin-3 and is more abundant in type 1 than in type 2 fibers. J. Lipid Res. **45:**603–609.
55. **Weyer, C., J. E. Foley, C. Bogardus, P. A. Tataranni, and R. E. Pratley.** 2000. Enlarged subcutaneous abdominal adipocyte size, but not obesity itself, predicts type II diabetes independent of insulin resistance. Diabetologia **43:**1498–1506.
56. **Yagyu, H., G. Chen, M. Yokoyama, K. Hirata, A. Augustus, Y. Kako, T. Seo, Y. Hu, E. P. Lutz, M. Merkel, A. Bensadoun, S. Homma, and I. J. Goldberg.** 2003. Lipoprotein lipase (LpL) on the surface of cardiomyocytes increases lipid uptake and produces a cardiomyopathy. J. Clin. Investig. **111:**419–426.
57. **Yang, L., H. C. Dan, M. Sun, Q. Liu, X. M. Sun, R. I. Feldman, A. D. Hamilton, M. Polokoff, S. V. Nicosia, M. Herlyn, S. M. Sebti, and J. Q. Cheng.** 2004. Akt/protein kinase B signaling inhibitor-2, a selective small molecule inhibitor of Akt signaling with antitumor activity in cancer cells overexpressing Akt. Cancer Res. **64:**4394–4399.
58. **Zou, Z., C. C. DiRusso, V. Ctrnacta, and P. N. Black.** 2002. Fatty acid transport in *Saccharomyces cerevisiae*. Directed mutagenesis of FAT1 distinguishes the biochemical activities associated with Fat1p. J. Biol. Chem. **277:**31062–31071.